

# Variation of Heating Efficiency of Magnetically Sheared CHS Plasmas by Polarization Control of 106GHz EC-Wave

YOSHIMURA Yasuo, AKIYAMA Tsuyoshi, ISOBE Mitsutaka, SHIMIZU Akihiro, SUZUKI Chihiro, TAKAHASHI Chihiro, NAGAOKA Kenichi, NISHIMURA Shin, MINAMI Takashi, OKAMURA Shoichi, MATSUOKA Keisuke, KUBO Shin, SHIMOZUMA Takashi, NOTAKE Takashi and OHKUBO Kunizo

*National Institute for Fusion Science, Toki 509-5292, Japan*

(Received: 9 December 2003 / Accepted: 20 May 2004)

## Abstract

To clarify the effect of polarization on electron cyclotron heating (ECH) in magnetized plasmas, experiment controlling the polarization of injected EC-waves is carried out in Compact Helical System (CHS). In the experiment, plasmas are generated and sustained only with 106.4 GHz ECH power. Magnetic field at the magnetic axis is 1.9 T so that the wave frequency is second harmonic. The optimum direction of linear polarization for the shortest time-delay of density start-up from the start of power injection and the optimum direction for the highest electron temperature and plasma stored energy during plasma duration show clear difference. The difference is attributed to the CHS magnetic configuration with strong shear and the plasma volume expansion from magnetic axis to the last closed flux surface.

## Keywords:

ECH, helical system, polarization, heating efficiency, magnetic shear

## 1. Introduction

For localized deposition of ECH power in magnetized plasmas, which is one of the most important features of ECH, control of polarization of injected EC-waves is key issue [1]. For example, the best polarization for the second harmonic ECH (X-mode) differs 90 degrees from that for the fundamental ECH (O-mode). However, for plasmas with strong magnetic shear, the direction of linear polarization corresponding to X- or O-modes varies for different positions in plasmas. In devices with externally given strong magnetic shear such as stellarators, this effect is a matter of importance so that experiments concerning with the shear effect have been carried out for both ECH [2] and electron cyclotron emission (ECE) [3]. In both cases it is pointed out that in magnetically sheared configuration, behavior of polarization state of EC-waves in plasmas must be taken into account for effective ECH or ECE signal detection.

Also in Compact Helical System (CHS), a polarization control experiment was performed using 106.4 GHz ECH power and a polarizer on the power transmission line. The result is described in this paper with the outline as follows. In Sec. 2, CHS device and ECH system are described. Results of the polarization control experiment are shown in Sec. 3.

Calculations for power absorption related to polarization are carried out and compared with the experimental results in Sec. 4. Finally, conclusions are stated in Sec. 5.

## 2. CHS device and ECH system

CHS is one of the helical devices with toroidal period number  $m = 8$  and polarity  $l = 2$ . Major radius of CHS plasma is about 1.0 m and the averaged minor radius is 0.2 m so that the aspect ratio is 5. The position of the magnetic axis  $R_{ax}$  can be shifted around 1.0 m and the magnetic field at plasma axis  $B_{ax}$  can be varied up to 2.0 T. The experiments described in this paper are carried out with  $R_{ax}$  of 0.92 m and  $B_{ax}$  of 1.9 T so that the magnetic axis lies on second harmonic resonance layer for waves with frequency of 106.4 GHz.

Magnetic field structure with rotational transform for plasma confinement is generated totally by external coils such as a couple of helical coils and three pairs of poloidal coils. The rotational transform increases with plasma minor radius. The poloidal component of magnetic field near the magnetic axis is nearly zero and it becomes comparable to the toroidal component at peripheral region.

Figure 1 shows a schematic view of the poloidal cross section at the beam injection port. It is so-called horizontally

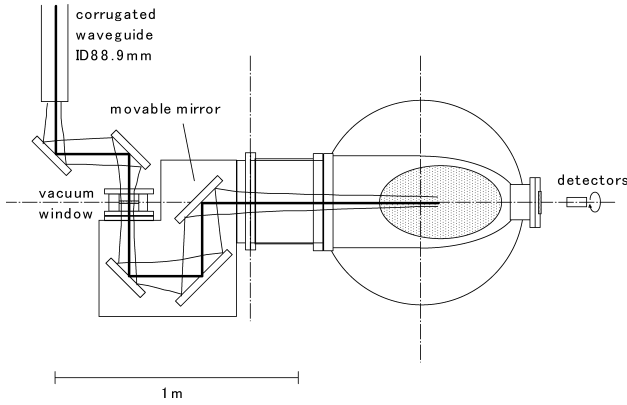


Fig. 1 A schematic view of the poloidal cross section at the EC-wave power injection port.

elongated cross section. The EC-wave beam propagates on the equatorial plane. The beam path is normal to the flux surface and parallel to the density gradient so that the beam refraction effect is minimized.

The strength of magnetic field along the beam path  $x$  is plotted in Fig. 2 with the angle between magnetic field direction and toroidal direction. Here, the origin of  $x$  corresponds to the magnetic axis. The right side of toroidal direction looking from outside of the torus is defined as 0 degree and the angle is counted as counter-clockwise. At the last closed flux surface (LCFS) ( $x = -0.27$  m) closer to the beam injection mirror, the angle is 30 degrees and at the opposite side on the LCFS ( $x = 0.23$  m), it is  $-40$  degrees. The large magnetic shear is one of the distinguished features of helical systems compared with tokamaks.

ECH system is constructed with a 106.4 GHz gyrotron, corrugated waveguide transmission line, a set of matching mirrors connecting the beam between gyrotron and waveguide, and injection focusing mirrors. The injection power to CHS vacuum vessel and the pulse length are kept at 130 kW and 30 ms, respectively in the experiment.

One of the matching mirrors is a grating polarizer with the groove depth of 0.7 mm, that is,  $1/4$  of the wavelength of the beam. The angle between the incident beam direction and the normal of the polarizer disc is only 7.2 degrees so that it is considered as an ideal polarization rotator. The controllability of polarization is the key point of the experiment then the characteristic of the polarizer is confirmed with real gyrotron power. At the opposite port to the injection port, two mm-wave power detectors are set on the extension of the beam path outside of a vacuum window, see Fig. 1. Each detector is sensitive to orthogonal directions of polarization then rotating the set of detectors around the beam path, polarization direction of injected wave can be determined by short pulse power injection to the vacuum vessel without generating plasmas.

The injection focusing mirrors are designed so that the beam profile is circular gaussian with waist size ( $1/e$  radius of electric field amplitude) of 15 mm. By IR-camera

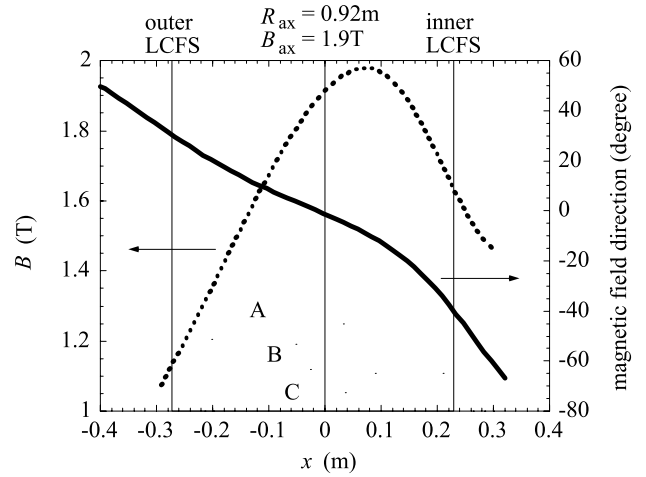


Fig. 2 The strength of magnetic field and the angle between magnetic field direction and toroidal direction along the beam path are plotted. The beam comes from negative  $x$  side. The curves marked as A, B show schematic profiles of  $n_e$  and  $T_e$  respectively used in latter calculations for heating phase, and C,  $n_e$  and  $T_e$  for break down phase.

measurement, it is confirmed that the real beam is close to the designed one: the beam has a size of  $17.5 \times 19.7$  mm at the magnetic axis. The beam size is small enough to determine the magnetic field direction at the localized power deposition region in complicated 3-D structure of magnetic field in CHS.

### 3. Polarization control experiment

In the experiment, plasmas are generated and sustained only with ECH power to simplify the situation. All the setting parameters such as magnetic field, gas-fueling except for the polarization direction of injected EC-wave power,  $\theta_{pol}$ , is fixed.  $\theta_{pol}$  is defined with the same manner of definition of the magnetic field direction plotted in Fig. 2. After some time delay from the start of power injection, density and stored energy rise up. Here the time delay of density start up  $t_{delay}$  is taken as a measure of optimization of plasma break down. The maximum stored energy  $W_{max}$  and the highest central electron temperature  $T_{e0max}$  achieved during plasma duration are considered as measures of optimization of plasma heating. At the early phase of plasma shot, electron temperature is rather low and the density has a peaked profile around the magnetic axis. After that the temperature becomes high and the density profile becomes broad as measured with Thomson scattering measurement.

In Fig. 3,  $t_{delay}$ ,  $W_{max}$  and  $T_{e0max}$  are plotted as functions of  $\theta_{pol}$ . It is easily seen that the tendency of  $t_{delay}$  is different from others.  $t_{delay}$  is nearly symmetric around  $\theta_{pol} = 90$  degrees. With  $\theta_{pol}$  of less than 20 degrees and larger than 160 degrees, plasma can not be generated within the pulse length of 30 ms with the power of 130 kW. Plasmas start up earliest with  $\theta_{pol}$  of around 90 degrees. At the beginning of plasma break down with 2nd harmonic heating, plasma volume is

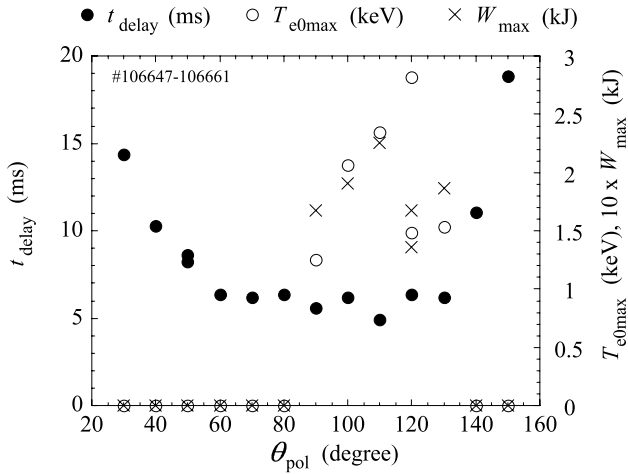


Fig. 3 The time delay of density start up  $t_{delay}$  (closed circle), the maximum stored energy  $W_{max}$  (cross) and the highest central electron temperature  $T_{e0max}$  (open circle) achieved during the plasma duration are plotted as functions of the polarization direction  $\theta_{pol}$ . Here,  $W_{max}$  is multiplied by 10 for convenience.

restricted around the magnetic axis so that power injection with  $\theta_{pol} = 90$  degrees results in direct X-mode heating around magnetic axis.

On the other hand,  $W_{max}$  and  $T_{e0max}$  have peaks around  $\theta_{pol} = 120$  degrees. Plasmas can not be effectively heated with  $\theta_{pol}$  of less than 80 degrees though density is risen up. This result is understood as follows. Electromagnetic waves injected to vacuum vessel start coupling with plasmas at the plasma boundary and, as waves in plasmas, propagate basically keeping its property as X- or O-mode waves when the characteristic lengths of variation of magnetic field or density are larger than wave length. Considering the direction of magnetic field of 30 degrees at plasma boundary,  $\theta_{pol} = 120$  degrees results in the maximum coupling as X-mode wave then efficient X-mode heating at the magnetic axis is realized.

#### 4. Confirmation of the experimental results by calculations

In this chapter, calculations to confirm the results taking the CHS magnetic configuration into account are described. Equations representing the relation between the X- and O-mode waves during their propagation in sheared plasmas [4]:

$$\frac{d^2 E_{//}}{dx^2} + \left( \frac{\omega^2}{c^2} N_O^2 - \phi^2 \right) E_{//} = 2\phi \frac{dE_{\perp}}{dx} + \frac{d\phi}{dx} E_{\perp},$$

$$\frac{d^2 E_{\perp}}{dx^2} + \left( \frac{\omega^2}{c^2} N_X^2 - \phi^2 \right) E_{\perp} = -2\phi \frac{dE_{//}}{dx} - \frac{d\phi}{dx} E_{//}$$

are numerically calculated considering power absorption effect at resonance region. Here,  $E_{//}$  and  $E_{\perp}$  are parallel and perpendicular components of wave's electric field to magnetic field.  $N_o$  and  $N_x$  denote the refractive indices of O- and X-

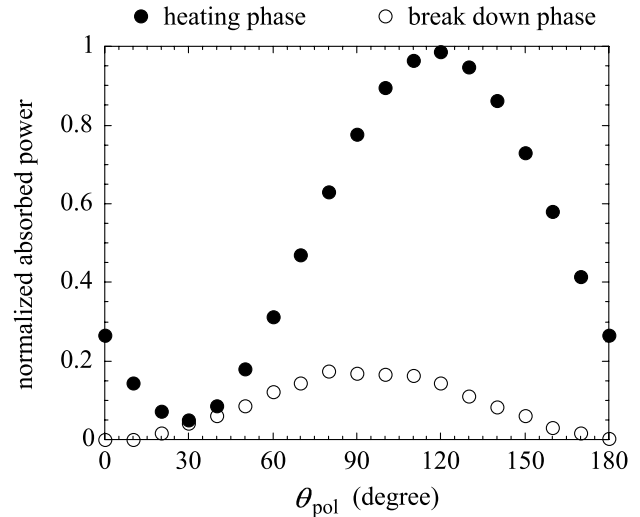


Fig. 4 Calculations of total absorbed power with various directions of linear polarization  $\theta_{pol}$  are plotted taking the injection power as unity. For the calculation of the break down phase, localized profiles of temperature and density around the magnetic axis, and for the heating phase nearly flat density profile and peaked temperature profile are adopted, respectively.

mode waves, and  $x$ : distance along the beam path,  $\phi$ :  $x$ -differential of magnetic field direction (magnetic shear),  $\omega$ : angular frequency of the wave,  $c$ : light speed, respectively. Using these equations the mixing effect of the two modes caused by the magnetic shear can be treated. To simulate the early phase of plasma break down and heating phase at the latter of plasma duration, two sets of density and temperature profiles are used. For the break down phase, localized profiles around the magnetic axis with the center values  $n_{e0}$  and  $T_{e0}$  of  $0.5 \times 10^{13}/\text{cm}^3$  and  $0.2$  keV are adopted. For the heating phase, much broadened, nearly flat density profile and peaked temperature profile with  $n_{e0}$  and  $T_{e0}$  of  $2.0 \times 10^{13}/\text{cm}^3$  and  $2.0$  keV are used. Those profiles are schematically seen in Fig. 2.

Total absorbed power calculated with various directions of linear polarization  $\theta_{pol}$  are plotted in Fig. 4. The absorbed power is normalized taking the injection power as unity. The absorbed fraction is not so much for the break down phase but clear peak around  $\theta_{pol} = 90$  degrees is recognized. The highest absorption for the heating phase by setting  $\theta_{pol}$  as 120 degrees is also confirmed. In the calculations, the density and temperature are fixed for each case. In the real process in the interaction of EC-waves with plasmas, nonlinear effects due to the progress of plasma parameters play an important role. The nonlinear effects result in the stronger dependence of temperature and stored energy on  $\theta_{pol}$  in the experiment compared with the calculated absorbed power fraction.

#### 5. Conclusions

In CHS, experiment investigating the variation of heating efficiency concerning with the polarization of EC-waves is

carried out. To realize effective 2nd harmonic X-mode heating at the magnetic axis, setting the polarization of injected wave to be perpendicular to the magnetic field at the magnetic axis is not sufficient, though it is most efficient for plasma break down. Highest electron temperature and plasma stored energy are achieved with the polarization perpendicular to the magnetic field near plasma boundary. Propagating process of X- and O-mode waves in the case of propagation perpendicular to flux surfaces, where the waves nearly keep its property during propagation in magnetically sheared plasmas, is clearly confirmed. Calculations taking the magnetic field structure of CHS support the experimental

results. It shows that the highest absorption efficiency for plasmas expanded to LCFS is achieved with the polarization perpendicular to the magnetic field near the LCFS while that for plasmas localized around magnetic axis is achieved with the polarization perpendicular to the magnetic field at the magnetic axis.

### References

- [1] for example, M. Bornatici, *Phys. Plasmas* **24**, 629 (1982).
- [2] K. Nagasaki *et al.*, *Phys. Plasmas* **6**, 556 (1999).
- [3] P.C. de Vries *et al.*, *Phys. Plasmas* **7**, 3707 (2000).
- [4] I. Fidone and G. Granata, *Nucl. Fusion* **11**, 133 (1971).